communications physics

A Nature Portfolio journal

Perspective

https://doi.org/10.1038/s42005-025-02476-5

# The CRESST experiment towards the next generation of sub GeV direct dark matter detection



G. Angloher[1], S. Banik[2,3], A. Bento[1,11], A. Bertolini[4], R. Breier[5], C. Bucci[6], J. Burkhart[2], L. Canonica[1,12], F. Casadei[1], E. R. Cipelli[1], S. Di Lorenzo[1,6], J. Dohm[7], F. Dominsky[1] ✉, L. Einfalt[2,3,13,14], A. Erb[8,15], E. Fascione[4], F. V. Feilitzsch[8], S. Fichtinger[2], D. Fuchs[2,3], V. M. Ghete[2], P. Gorla[6], P. V. Guillaumon[1,16] ✉, D. Hauff[1], M. Ješkovský[5], J. Jochum[7], M. Kaznacheeva[8], H. Kluck[2], H. Kraus[9], B. V. Krosigk[4,10] ✉, A. Langenkämper[1], M. Mancuso[1], B. Mauri[1], V. Mokina[2] ✉, C. Moore[1], P. Murali[4], M. Olmi[6], T. Ortmann[8], C. Pagliarone[6,17], L. Pattavina[6,12], F. Petricca[1], W. Potzel[8], P. Povinec[5], F. Pröbst[1], F. Pucci[6], F. Reindl[2,3], J. Rothe[8], K. Schäffner[1], J. Schieck[2,3], S. Schönert[8], C. Schwertner[2,3], M. Stahlberg[1], L. Stodolsky[1], C. Strandhagen[7], R. Strauss[8], I. Usherov[7], D. Valdenaire[2,3], M. Zanirato[1] & V. Zema[1,2]

Direct detection experiments have established the most stringent constraints on potential interactions between particle candidates for relic, thermal dark matter and Standard Model particles. To surpass current exclusion limits a new generation of experiments is being developed. The upcoming upgrade of the CRESST experiment will incorporate $\mathcal{O}(100)$ detectors with different masses ranging from ~2 g to ~24 g, aiming to achieve unprecedented sensitivity to sub-GeV dark matter particles with a focus on spin-independent dark matter-nucleus scattering. This paper presents a comprehensive analysis of the planned upgrade, detailed experimental strategies, anticipated challenges, and projected sensitivities. Approaches to address and mitigate low-energy excess backgrounds – a key limitation in previous and current sub-GeV dark matter searches – are also discussed. In addition, a long-term roadmap for the next decade is outlined, including other potential scientific applications.

Since the 1930s, significant efforts have been made to understand the nature of dark matter (DM) with experimental searches for DM particles starting to gain momentum in the 1980s. DM particle candidates span a mass range of about 50 orders of magnitude, from about $10^{-22}$ eV up to the Planck scale. For decades, weakly interacting massive particles (WIMPs), generated thermally during the hot, early universe, have been one of the most studied DM candidates[1]. Of these, the most prominent role over the years has been played by a WIMP with a mass above a few GeV/$c^2$ and below a few hundred TeV/$c^2$, often referred to as standard WIMP[2,3]. However, theoretically well-motivated WIMP models with sub-GeV masses also exist, commonly called light DM. The latter have been gaining increasing attention in recent years due to the lack of a standard WIMP observation to date[4,5]. Over the past 40 years, a variety of approaches, techniques, and experiments have been employed to tackle this complex puzzle. Among them, the Cryogenic Rare Event Search with Superconducting Thermometers (CRESST) experiment has been a key player for over 20 years, advancing the direct search for WIMPs with masses of a few GeV/$c^2$ and later extending below 1 GeV/$c^2$, using cryogenic calorimetry.

The CRESST experiment began acquiring data in the INFN Laboratori Nazionali del Gran Sasso (LNGS, Italy) in 2000, initially using sapphire ($Al_2O_3$) crystals[6]. Currently in its third phase, the experiment operates cryogenic calorimeters made from crystalline materials such as $Al_2O_3$, $CaWO_4$[7], Si[8], and $LiAlO_2$[9] equipped with highly sensitive transition-edge sensors (TESs) operated at ~15 mK. The main goal of the experiment is to discover DM, an effort that is still ongoing. In the meantime, CRESST has been able to probe DM candidates with spin-independent DM-nucleon scattering cross sections down to $\mathcal{O}(10^{-42})$ $cm^2$ at 10 GeV/$c^2$[10]. Thanks to the low thresholds achieved by this technology, as low as 6.7 eV for gram-scale detectors[11] and 30.1 eV for a 23.6 g crystal[10], CRESST has additionally successfully probed sub-GeV DM with spin-independent DM-nucleon scattering cross sections down to $\mathcal{O}(10^{-38})$ $cm^2$ at 1 GeV/$c^2$ and masses as low as 73 MeV/$c^2$[10–12]. Further remarkable results that have been achieved

A full list of affiliations appears at the end of the paper. ✉e-mail: dominsky@mpp.mpg.de; pedro.guillaumon@mpp.mpg.de; bkrosigk@kip.uni-heidelberg.de; valentyna.mokina@oeaw.ac.at

both in terms of technological advancements and particle physics include single-photon detection capabilities using a silicon-on-sapphire (SOS) cryogenic detector[11], and the first measurement of the $^{180}$W $\alpha$-decay, with a half-life of $1.8(2) \times 10^{18}$ years[13]. In addition to the achievable thresholds, another notable advantage of the CRESST technology is its flexibility in the target material, allowing the use of nuclei sensitive to both SI and SD couplings[9–11].

With well-established technology, CRESST is ready to embark on a comprehensive upgrade. This new phase will feature 288 readout channels, significantly increasing the achievable exposure, with the aim of unprecedented sensitivity in sub-GeV DM searches reaching a scattering cross section of $\mathcal{O}(10^{-42})$ $cm^2$ at 1 GeV/$c^2$. Although the primary goal of CRESST is to probe new DM parameter space for elastic DM-nucleus scattering in the sub-GeV range, it will also enable investigations into other intriguing physics cases, including searches for solar axions[14], axion-like particles (ALPs)[15], dark photons[16] and constraints on self-interaction cross-sections of dark matter in universal bound states[17]. However, this upgrade presents several challenges. The large number of low-temperature detectors with TESs and Direct Current Superconducting Quantum Interference Devices (DC-SQUIDs) readout introduces additional complexity in the setup. A reformulation of the data processing pipeline is underway to handle the increased data rate and to automate the optimization of detector operational conditions including bias current using reinforcement learning[18]. First-level quality and live-time cuts, with substantial machine learning efforts are foreseen[19] along with the adaptation of existing simulation techniques to efficiently model the entire setup. The new approach will use the likelihood normalization method[20] from the current background model while minimizing the time required for simulations, analysis, and model development.

The original plans for this upgrade have been delayed by the discovery of an increased background event rate below ~200 eV, which was first reported by CRESST-III in 2019. This phenomenon is now known as the Low-Energy Excess (LEE)[10]. A comparable LEE was soon also reported by other low-threshold experiments employing different detection techniques and/or target materials[21–23]. The scientific community is making considerable efforts to understand and mitigate this excess, which hampers sensitivity to light DM. To address the LEE, the collaboration has developed new detector layouts[24–26], launching dedicated measurement campaigns, the most recent of which began in 2024.

## The CRESST experiment

In 1993, the Technical University Munich and the Max-Planck Institute for Physics initiated a collaboration to develop a DM search experiment called "Munich Dark Matter Search" using cryogenic calorimeters with TESs at LNGS[27]. In 1996, the experiment was renamed "CRESST" as the collaboration expanded to include teams from the University of Oxford and LNGS.

The experiment, which was first located in hall B of LNGS, performed its first DM search in 2000 using four $Al_2O_3$ detectors with a mass of ~260 g each. The results from this initial phase, later known as CRESST-I, set the best limits on spin-dependent and independent interactions for DM particles with a mass around 1 GeV/$c^2$ at that time[6]. However, high backgrounds prompted the collaboration to work on an improvement plan. To actively distinguish between background and potential DM signals a double readout scheme was developed, marking the transition to CRESST-II, based on the use of scintillating crystals as targets for the DM interaction, paired with much smaller cryogenic calorimeters (light detectors) for the detection of the scintillation light emitted by the main crystal. Several different scintillating crystals were tested and the prominent interest at that time for DM in the 100 GeV/$c^2$ mass range motivated the selection of $CaWO_4$ scintillating crystals, given the content of the heavy tungsten nuclei, a spin-independent scattering cross sections that scales with the square of the atomic mass number[5]. After moving the setup to hall A, the first results obtained in 2004 with two ~ 300 g $CaWO_4$ detectors showing a strong suppression of non-nuclear recoil backgrounds were published[28].

Subsequent upgrades of the electronics system enabled the operation of several detector modules (scintillating crystal and corresponding light detector) simultaneously, with first results published in 2007[29] and a more extensive measurement campaign concluding in 2011[30]. This campaign suffered from background events due to alpha decays on the surfaces facing the detectors, which was addressed by redesigning the detectors' holding structure. The results of the detector with the best performance with this improved holding in CRESST-II were published in 2014[31].

With increased theoretical interest in light DM candidates, CRESST shifted its focus in order to explore a region of the parameter space for elastic, spin-independent DM-nucleon scattering corresponding to WIMP masses below a few GeV/$c^2$[32]. This phase of the experiment, called CRESST-III, further optimized the detector layout using smaller $CaWO_4$ crystals to lower the detection threshold, and reduced the background by enhancing the radiopurity of the crystals. The first results with the optimized detectors that achieved a threshold of 30.1 eV were published in 2019. This unmatched threshold for massive calorimeters extended the detection sensitivity to DM masses as low as 160 MeV/$c^2$[10]. However, in this phase the experiment's sensitivity was limited by the appearance of LEE events near the detection threshold. In CRESST-III, also other target materials were introduced, such as $Al_2O_3$ and $LiAlO_2$ (better suited for the search for light DM and spin-dependent interactions), and new detector designs were developed to investigate the origin of the LEE.

### Working principle

Typically, CRESST utilizes a scintillating crystal as a target material, measuring both a heat (phonon) signal and a scintillation light (photon) signal. When a particle interacts with the target, nearly all the deposited energy (~90%) is transferred to the crystal as phonons, a percentage that remains largely independent of the type of interaction. Therefore, the phonon signal represents the energy deposited by the interacting particle, though it does not provide information about the particle's identity. The scintillation light signal, however, is highly dependent on the interacting particles. For beta/gamma interactions, leading to electron recoils, the emitted light in $CaWO_4$ accounts for no more than 7% of the observed energy. The scintillation light emitted for nuclear recoils is significantly reduced due to quenching, making it roughly an order of magnitude lower[33]. Both the phonon and light signals are simultaneously measured by separate thermometers, and the ratio between the energy deposited in these two channels, known as the light yield (LY), is determined.

The LY allows differentiation between particle interactions. As shown in Fig. 1, beta/gamma interactions exhibit the highest light yield, while the LY of nuclear recoils from Oxygen (O), Calcium (Ca), and Tungsten (W) is significantly lower. These recoils can be induced by either neutrons, neutrinos or DM particles. At energies above about 2 keV, electromagnetic background events, primarily within the beta/gamma bands, are easily distinguishable from nuclear recoils. At lower energies, which are of particular interest for light DM searches, the beta/gamma bands, as defined in ref. 34, overlap with the nuclear recoil bands, making it difficult to distinguish between different particle interactions on an event-by-event basis. For this reason, CRESST is extensively working on the development of its background model[20,35] to continuously improve the identification of background components on a statistical basis, maintaining high sensitivity for light DM.

### CRESST setup

The experiment is situated beneath the Gran Sasso massif. The surrounding rock provides a cosmic radiation shield equivalent to 3800 meters of water[36]. To further reduce potential backgrounds, the experiment is protected by additional passive shielding and active veto layers. From the outermost to the innermost, these include a polyethylene (PE) layer, an active muon veto, a lead layer, a copper layer, and a second PE layer, as illustrated in Fig. 2. The shielding layers inside the muon veto are enclosed in an air tight container (radon-box) which is constantly flushed with $N_2$ gas and maintained at a slight overpressure in order to prevent radon accumulation near the

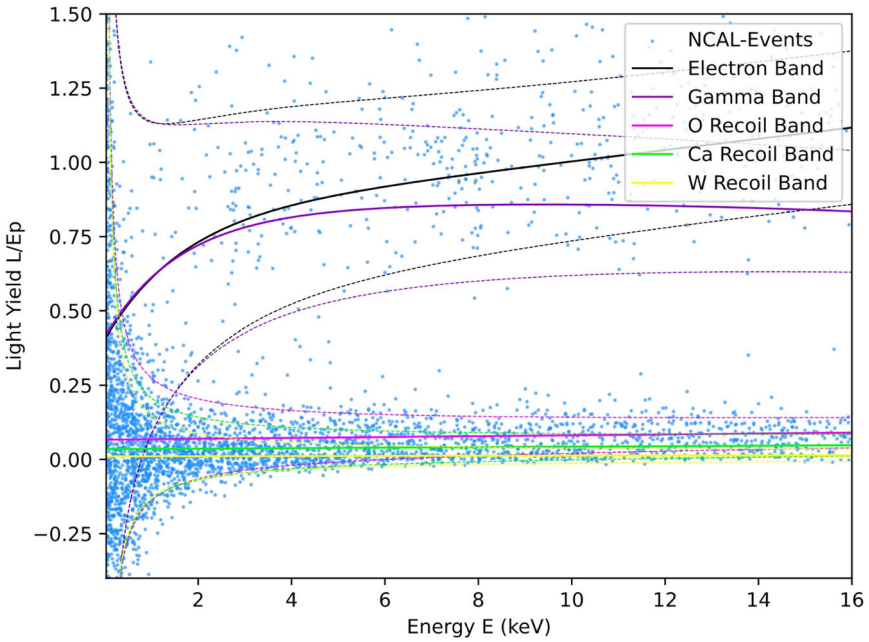


**Fig. 1 | Light yield as a function of phonon energy.** Fitted electron (black), gamma (purple), oxygen (magenta), calcium (green) and tungsten (yellow) bands in the light yield (i.e., the energy of the light signal $L$ over the energy of the phonon signal $E_p$) versus energy plane for the neutron calibration data acquired with Detector A—a CRESST-III detector module with a $CaWO_4$ crystal target (taken from supplementary files of ref. 34).

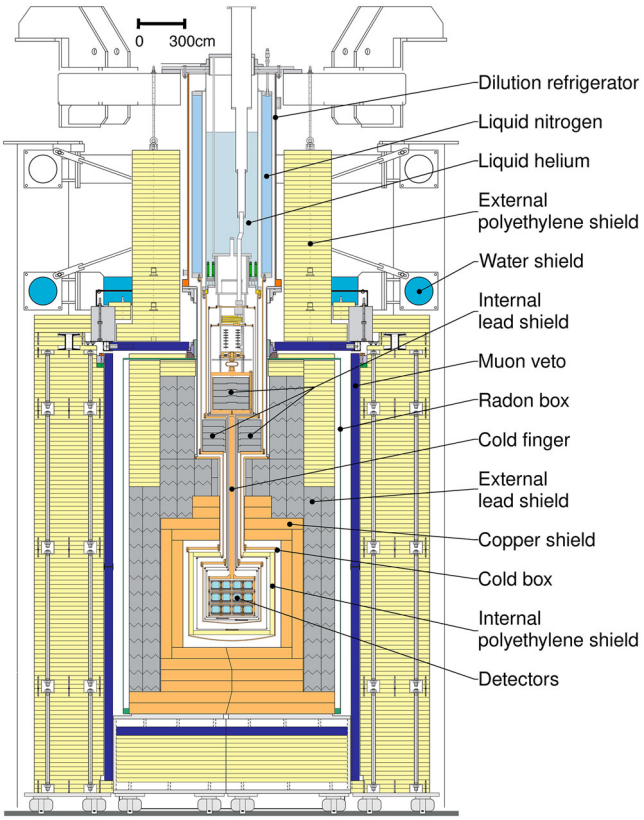


**Fig. 2 | Schematic view of the CRESST setup.** The illustration depicts the main components of the CRESST experimental setup, including successive layers of passive and active shielding. From the outermost to the innermost regions, the setup features polyethylene, a muon veto system for background suppression and lead shields, a copper shield. The cryogenic infrastructure—comprising the dilution refrigerator, cold box, and cold finger—houses the detector modules. Liquid nitrogen and liquid helium circuits provide the required cooling stages.

detectors. The PE shields against environmental neutrons. The muon veto, covering 98.7% of the experiment's outer surface, identifies muons, allowing for the rejection of muon-induced events. The experiment is shielded from gamma radiation by 20 cm of lead, weighing 24 t, which effectively absorbs gamma rays due to its high atomic number and density. Within the lead shielding, there is a 14 cm thick layer consisting of 10 t of radiopure copper layer. An additional PE layer inside the experimental volume shields the detectors from neutrons produced by interactions in the lead and copper. To minimize the radioactive background, all materials used around and within the detectors are carefully selected based on their radiopurity.

The cooling to the operational temperature of $\mathcal{O}(15)\,mK$ is achieved using a commercial $^3He/^4He$ dilution refrigerator. The cryostat and the dewars containing cryogenic liquids do not extend into the low background experimental volume (cold box), ensuring that there is no direct line of sight between the non-radiopure dilution refrigerator and the detectors. The low temperature of the dilution refrigerator is brought into the cold box via a 1.5 m long cold finger. The cold box consists of five concentric radiation shields that surround the experimental volume and the cold finger. The cold finger and the shields are made of radiopure copper.

## Detector module

A typical CRESST detector module consists of a (scintillating) target crystal, a light detector, and a reflective and scintillating housing. Following an energy deposition in the target crystal, a phonon signal is detected using a TES, a thin tungsten film deposited on a thin layer of amorphous $SiO_2$ which is placed directly on the crystal. The TES is operated at ~15 mK, where tungsten is in the transition to its superconductive state. When phonons are absorbed by the TES, they raise its temperature, causing a measurable change in resistance. The resulting change in current through an inductance coil alters the magnetic flux, which is measured by a SQUID amplifier. To detect the light emitted by the scintillating target crystal, a 0.4 mm thin SOS wafer equipped with a TES is used as a cryogenic light detector, also read out by a SQUID amplifier.

In the first run of CRESST-III (2016–2018), the detector modules were modified from those in CRESST-II, resulting in a detection threshold 10 times lower: Detector A, with a 23.6 g block-shaped $CaWO_4$ crystal measuring $20 \times 20 \times 10\ mm^3$, had by that time the lowest threshold of 30.1 eV[10]. The target crystal and the light detector were held by three 12 mm $CaWO_4$ sticks (each) and placed in a copper housing lined with reflecting and scintillating Vikuiti® foil. This created a fully scintillating housing which

allows to efficiently veto recoil events from alpha decays on surfaces or surface-near layers of materials surrounding the crystal[31,37]. The detector and its schematic view are presented in Fig. 3.

Currently, the CRESST experiment tests in different runs a variety of detector modules, each exhibiting distinct configurations[22,26]. These variations include the use of target materials other than $CaWO_4$ in certain modules, as well as differing crystal holding mechanisms, applying either bronze clamps or copper sticks and gravity-based approaches. These modifications are systematically implemented to investigate potential sources of the LEE.

## Current status

As mentioned in section "Introduction", the LEE refers to a steeply increasing event rate (below about 200 eV in the CRESST data) towards decreasing recoil energies which has been observed in all cryogenic low-background experiments with a low enough threshold[21,23]. This excess cannot be explained by a DM signal, known particle-induced background sources, or noise fluctuations large enough to trigger the detector[22,23]. The CRESST experiment first observed the LEE during the CRESST-III operations in Detector A[10]. Other modules of the same run that achieved an energy threshold below 100 eV also showed an LEE, but the focus in the following will remain on the detector with the lowest threshold, i.e., Detector A. The energy spectrum observed in this detector is shown in Fig. 4. The CRESST-III phase of the experiment achieved world-leading exclusion limits on the spin-independent DM-nucleon cross section below about 1 GeV/$c^2$, reaching sensitivity to DM masses as low as 160 MeV/$c^2$ [10]. More recently, CRESST set new world-leading limits below 0.2 GeV/$c^2$, reaching down to a mass of 73 MeV/$c^2$ [11]. However, in both cases, the LEE overlaps with a large part of the DM search region in the recoil energy spectrum, significantly reducing the sensitivity to the cross section as will be detailed in section "Performance studies with upgraded setup and with LEE". Therefore, the identification, characterization and mitigation of the LEE has become the highest priority in recent years.

### Investigating the low-energy excess

The CRESST Collaboration has put significant effort into understanding the excess background through dedicated measurements. Different module designs were developed and tested, and focused analyses have been conducted, to isolate possible causes for this unexpected background, as will be laid out in this section. Tests have been carried out both at a surface facility and at the LNGS CRESST facility to avoid possible effects that are exclusive to measurements above ground or certain cryostats. The collective findings of these investigations show that the LEE is currently dominated by detector-intrinsic effects rather than a particle origin, aligning with the community-wide observations[22].

**Detector layout studies**. Extensive studies have been conducted with detector modules exploiting varying target materials, holding structures, and surrounding materials. Observations show that the LEE rate and spectral shape varies between detector modules and persists in non-scintillating materials, conflicting with an external origin such as luminescence, external radioactivity, or single-particle origins like DM. The following specialized detector designs have provided these crucial insights into the nature of the LEE and/or will help to further narrow down the detector-intrinsic phenomena causing the majority of the excess and enable vetoing of LEE events while maintaining a high signal efficiency[24–26]:

1. **DoubleTES Detectors**: These modules employ two identical TESs, on the target crystal to distinguish between events occurring within the absorber bulk and those at or near the TESs, plus a light detector. Initial studies reveal that a component of the LEE originates at or near one of the TESs, pointing towards interface effects as a source.
2. **Mini-Beaker Module**: This module features a 4$\pi$ veto and an instrumented holding structure designed to tag surface radiation and events from the surroundings. The cylindrical $Al_2O_3$ target crystal is surrounded by a silicon beaker and an $Al_2O_3$ ring, all instrumented with TESs. The veto channels significantly improve background tagging.
3. **Centimeter-Cube (cm-Cube) Array Module**: This design uses an array of four 1 $cm^3$ $CaWO_4$ crystals with a low-force holding scheme and two light detectors, one above and one below the absorbers. The small absorber size reduces energy thresholds, enhancing sensitivity to low-energy events. This module also allows for to study coincidences between the events.

**Time-dependence studies**. The LEE rate has been observed to decay over time, exhibiting two distinct time constants. The faster decay component partially resets after thermal cycles—specifically, after warming the detectors to tens of Kelvin—excluding a particle origin as the main source. Instead, a viable hypothesis that we proposed[38] and are testing via a DoubleTES module is that a mismatch between the thermal expansion coefficients of the crystal and the sensor induces shear stress at the interface, storing energy which can eventually be released contributing to the low energy excess events. Also, other collaborations consider this a plausible hypothesis[39]. In general, this time dependence suggests that the LEE rate can be significantly reduced by maintaining stable, long-term cryogenic conditions[22]. Above-ground detector tests reveal decay times for the LEE consistent with those observed underground, indicating a common origin that is independent of the location[24].

**Pulse shape studies**. Pulse shape analyses confirm that LEE events exhibit pulse shape characteristics indistinguishable from particle recoil events at the level of accuracy achievable with current technology[22]. This observation, together with the fact that the excess extends well above the energy threshold, rules out triggered noise fluctuations as the cause[40].

### Mitigation strategies and ongoing research

Building on the insights gained about the LEE thus far, mitigation strategies are being developed at the detector design, operations, and analysis levels. These efforts include but are not limited to an optimized choice of materials at the detector interfaces, discrimination between events occurring in the bulk of the detector and at the sensor interface, and the inclusion of the time dependent behavior of the LEE in the likelihood analysis. We also envision new detector designs optimized to match the thermal expansion coefficients of the interfaced materials. In parallel, investigations continue to deepen the understanding of the underlying physical processes, aiming to eliminate their cause. If it is not possible to fully eliminate the LEE, it is necessary to identify a physically motivated, analytical description that can be incorporated into the likelihood. As a last resort, a particularly simple and practical backup strategy takes advantage of the natural decay of the LEE rate over time. Projections suggest that ~450 days after the initial cool-down of the experimental setup, the LEE rate will have decreased by a factor of 10. A factor 100 reduction would be reached after 900 days. Previous long-duration runs of the CRESST experiment, along with other collaborations using comparable infrastructures (e.g., [41]), have established the feasibility of multi-year continuous cryostat operation at base temperature. This "waiting-time" strategy provides an effective means to reduce background levels even in the worst-case scenario where no further advancements in LEE mitigation are achieved, despite the tremendous progress in recent years.

## Upgrade plans

The ongoing CRESST efforts to enhance the DM sensitivity are focused on three primary developments: (i) improving the detector performance by achieving lower energy thresholds, (ii) exploring strategies to mitigate or eliminate the LEE, and (iii) increasing the exposure.

Currently, there are 24 working readout channels in CRESST, allowing the simultaneous operation of 12 standard CRESST modules or 8 DoubleTES modules. This strongly limits the achievable exposure. To exploit the increased sensitivity of future detector modules, larger exposures and thus an increased amount of readout channels are required. Combined with

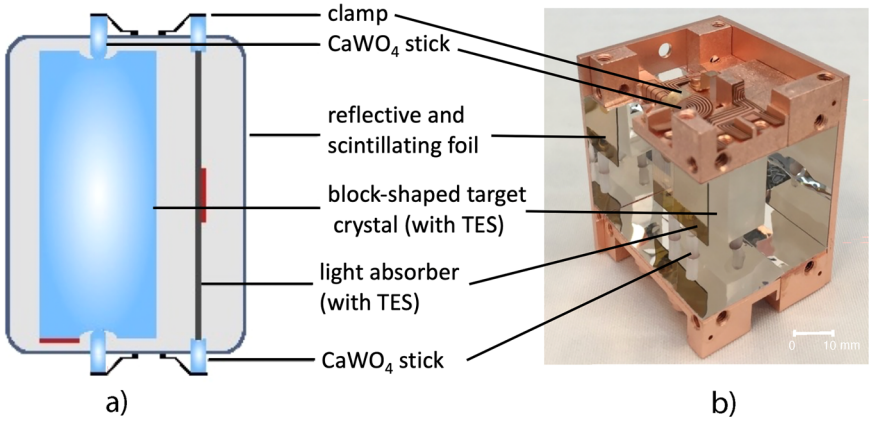


**Fig. 3 | CRESST-III detector module.** Schematic view (**a**) and photo (**b**) of a CRESST-III detector module. Parts in blue are $CaWO_4$, in red are the TESs. The block-shaped target crystal ($20 \times 20 \times 10$ mm$^3$) has a mass of 23.6 g. It is held by three $CaWO_4$ sticks. Three additional $CaWO_4$ sticks keep the light detector ($20 \times 20 \times 0.4$ mm$^3$) in place.

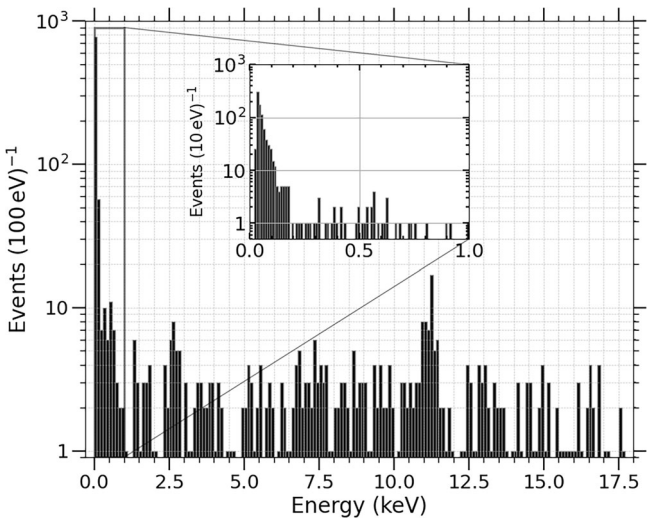


**Fig. 4 | Energy spectrum with the Low-Energy Excess.** Energy spectrum of Detector A[10] with an inset plot showing the Low-Energy Excess. The lines at 2.6 keV and 11.27 keV are from cosmogenic activation of $^{182}$W[43].

advancements in TESs, SQUIDs, and cabling even greater improvements are anticipated. To achieve a significant increase in sensitivity, the CRESST Collaboration foresees an upgraded readout system with 288 channels. The dilution refrigerator and current experimental facility in general are capable of supporting this upgrade. The upgraded configuration incorporates 288 DC-SQUIDs, installed on the 4.2 K flange within the liquid helium bath of the CRESST cryostat.

The entire data acquisition system and associated electronics will be upgraded, while maintaining the mechanical components of the setup. The collaboration has been developing an integrated detector operation and data acquisition system specifically for TES-based cryogenic detectors. These upgrades will provide the CRESST facility with state-of-the-art equipment, combining modern technological advancements with its robust and well-characterized infrastructure.

The detector layouts described in section "Current status", developed to study the origin of the LEE and to identify strategies for its mitigation, will also form the basis for the layouts for the next generation of CRESST. Due to the enhanced capability of the DoubleTES design to reject the component of the LEE originating from events in a single TES sensor, it is currently foreseen as the future baseline design. Further design optimizations are under consideration to enhance the sensitivity to sub-GeV DM while minimizing the LEE. The combination of these efforts is expected to lead to an improved sensitivity to light DM.

## Performance studies with upgraded setup and with LEE

The presence of the LEE has significantly limited the experiment's sensitivity to light DM, which is the primary focus of CRESST-III. To mitigate this excess and to increase the potential discovery to light DM, the collaboration is taking the two aforementioned approaches: The LEE background is being reduced by implementing improved module designs, and advanced analysis strategies are being developed to mitigate the remaining background. Based on recent advancements in detector development, an LEE reduction of a factor of 10–100 is deemed achievable. If none of the mitigation efforts fully eliminate the LEE, or at least significantly reduce it, the reduction factors of 10 and 100 are projected to be reached after ~1.5 and 3 years of continuous operation at base temperature, respectively. These two reduction factors are considered as benchmark values for CRESST upgrade sensitivity studies. A limit projection with the reduction factor of 10 for the LEE, while keeping the background level of Detector A[10] constant, was calculated using a likelihood framework[34,42]. The projection inherits the same 5.594 kg · day exposure as Detector A. In order to keep the spectral shape of the simulated data close to the observed spectrum, a simultaneous fit of the background and LEE is performed based on the method described in refs. 34,42. The LEE is modeled with an exponential function. The reduction is simulated by scaling the amplitude of the LEE, while all other backgrounds remain unchanged. A thousand Monte-Carlo simulations were performed from which the median and 1$\sigma$ band were extracted. The result is shown in Fig. 5 in comparison with the current experimental status of world-wide elastic, spin-independent DM-nucleon scattering searches. The implementation of a likelihood analysis framework[34] has already demonstrated enhanced sensitivity even in the presence of the LEE and without including its time dependence. In the case of a LEE reduction by a factor of ten for Detector A, the likelihood analysis is expected to improve by a factor of five compared to the Yellin method. Currently the likelihood results in weaker limits than the Yellin method because the latter is designed to deal with unknown backgrounds while likelihood methods rely on an accurate model of all signal and background components present in the data. Thus, a more accurate description of the excess could lead to significantly improved limits. Incorporating a time-dependent LEE model in the likelihood has the potential to further tighten the limits for sub-GeV DM even in the absence of any other excess mitigation.

### Primary science potential of the upgraded setup

In the following subsections, potential configurations and design choices are being discussed for the detectors in the upgraded CRESST setup. This includes a consideration of various absorber materials, module arrangements, and readout channel allocations, all aimed at optimizing the setup's performance for enhancing the overall sensitivity to DM particles.

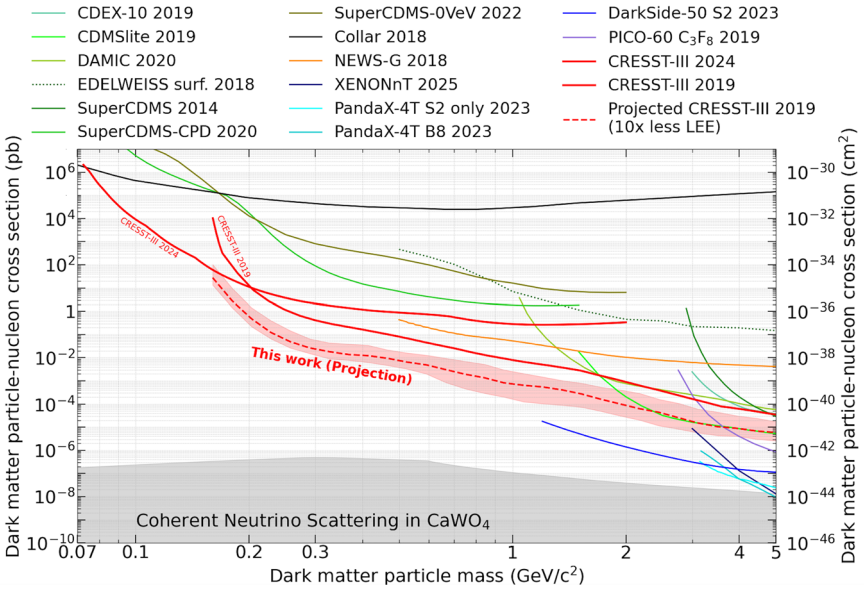


**Fig. 5 | Experimental results for elastic, spin-independent DM-nucleus scattering versus DM particle mass.** Unless explicitly stated otherwise, the results are reported with a 90% confidence level (two-sided). This work presents CRESST-III results in red: with SOS (CRESST-III 2024)[11], with $CaWO_4$ "Detector A" (CRESST-III 2019)[10] both as solid lines, and the median of a projection of Detector A with an assumption of 10 time less LEE as a red dashed line. The band represents the 1$\sigma$ region. Color coding is used to categorize the experimental results: green represents exclusion limits (CDEX[49], CDMSlite[50], DAMIC[51], EDELWEISS[52], SuperCDMS[53], SuperCDMS-CPD[54], SupersCDMS-0VeV[55]) obtained using silicon- or germanium-based solid-state detectors. Blue and cyan corresponds to liquid noble gas experiments using argon or xenon (DarkSide[56], Panda-X S2 only[57], Panda-X B8[58] XENONnT[59]). Black solid corresponds to organic scintillators—Collar[60], orange solid denotes the gaseous spherical proportional counter NEWS-G ($Ne + CH_4$)[61], light violet represents the superheated bubble chamber experiment PICO ($C_3F_8$)[62]. The gray area highlights the so-called neutrino fog, calculated for $CaWO_4$ in[48].

**Spin-independent dark matter interaction**. As described above, the upgraded setup will include 288 readout channels. Assuming the CRESST modules will retain the DoubleTES configuration, each module requires two readout channels for the target crystal and one for light detection, accommodating up to 96 DoubleTES detector modules. Limit projections for spin-independent DM interactions are derived for a representative array comprising 70 modules equipped with 24 g $CaWO_4$ crystals with a threshold of 30.1 eV and 26 lighter modules of 2 g $CaWO_4$ with a threshold of 5 eV which are realistic and achievable performance targets for these modules, given the benchmark values obtained with similar detectors already operated in CRESST. The intrinsic background level of the $CaWO_4$ crystal used for calculating the projections is conservatively assumed to be the same as measured with Detector A. The background level in the low-energy range could be improved by almost one order of magnitude with respect to commercially available crystals by using our own improved crystal growth procedure and purifying the raw materials[43,44]. Acquiring data throughout the period of 3 years will result in an expected total exposure of up to 1.5 tonne day. However, assuming Detector A background levels, the experiment will be background limited after about 1 tonne day independent of the LEE. For this reason, an exposure of 500 kg · day is conservatively applied for the presented limit projections, obtained after about one year of data taking with the 70 larger modules and a live time of 80%. The 26 lighter modules are designed to achieve lower energy thresholds and to enhance the sensitivity to light DM. When operated alongside the 70 larger modules, these smaller detectors will contribute an additional annual exposure of about 15 kg · day.

Figure 6 presents the resulting limit projections for both sets of modules and for LEE (normalized by exposure) reduction factors of 10 and 100, as motivated earlier. The LEE background was modeled using a single energy-dependent exponential function constant in time. The energy-dependent signal survival probability in Detector A was determined during data analysis. To obtain a realistic estimate for the 2 g modules, the signal survival probability of Detector A was scaled to account for the lower threshold. For simplicity, identical cut efficiencies, acceptance regions, and energy resolutions were assumed across all detectors. The energy resolution at zero energy is set to one fifth of the threshold value for each module. The number of simulated events is scaled according to the respective exposure and follows a Poisson distribution. The strength of the LEE is parameterized by a multiplicative factor applied to the exponential function describing the LEE. For masses up to about 1 GeV/$c^2$, the low-threshold 2 g modules with an exposure of 15 kg · day provide the strongest exclusion sensitivity. These specialized detectors extend the experiment's sensitivity range to cover DM masses down to 60 MeV/$c^2$, significantly broadening the experimental reach. At higher masses, the large combined exposure of the 24 g modules yields superior exclusion power. To ensure the readability of the plot, the projections for the two sets of modules are shown only in the mass range where they exhibit leading sensitivity.

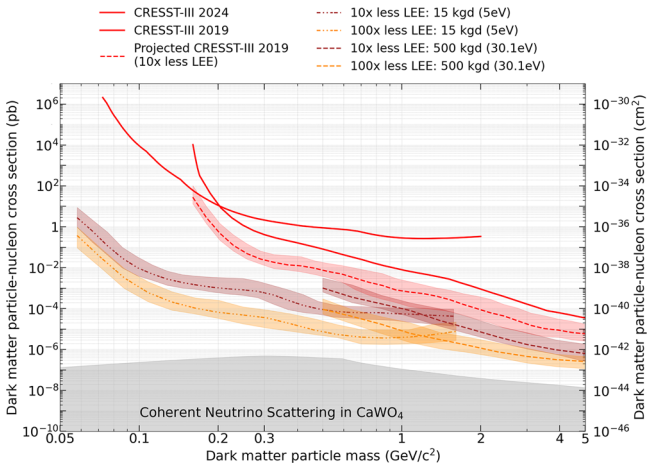


**Fig. 6 | Projected sensitivities at 90% confidence level (two-sided) on the elastic, spin-independent DM-nucleon scattering cross section.** The simulations are based on the Detector A performance exploring 26 $CaWO_4$ detectors with a threshold of 5 eV and an exposure of 15 kg · day (double dash double dotted) and 70 $CaWO_4$ detectors with a threshold of 30.1 eV and an exposure of 500 kg · day (dashed) for two reduction scenarios of the existing Detector A LEE (Excess): 10 times less LEE (in light burgundy color) and 100 times less LEE (in light orange color). For comparison, the limit for Detector A[10] (CRESST-III 2019, solid red line), the same limit but with 10% LEE (dashed red line), and the limit for the SOS detector[11] (CRESST-III 2024, solid red line) are shown. The bands represent the 1$\sigma$ region around the median. The gray area highlights the so-called neutrino fog, calculated for $CaWO_4$ in ref. 48.

**Spin-dependent dark matter interaction.** The CRESST experiment has previously demonstrated the sensitivity of lithium-based targets to spin-dependent interactions. Lithium, with its two isotopes, $^{6}$Li and $^{7}$Li, is particularly well-suited for these studies. It features unpaired protons and unpaired neutrons, making it sensitive to spin-dependent interactions with both protons and neutrons, and the model uncertainties on the nuclear structure with only few nucleons are comparatively small. In an earlier run, CRESST successfully operated two $LiAlO_2$ detector modules[9]. This configuration achieved leading limits on spin-dependent proton-only interactions for DM particle masses in the range of 0.25–2.5 GeV/$c^2$ showcasing the potential of lithium-based targets in the search for light DM. In the range of 0.074 to 0.25 GeV/$c^2$, CRESST SOS detectors[11] obtained leading limits, using $^{27}$Al as a probe to neutron-only interactions.

Building on this success, the upgraded CRESST setup will allow for the operation of a significantly larger number of $LiAlO_2$ detectors, substantially improving the sensitivity to spin-dependent interactions. The main background source for these detectors is the decay of tritium, which is produced through neutron capture on $^{6}$Li. Reducing this background will require significant efforts to prevent the lithium from exposure to neutrons from mining extraction to crystal production and detector operation. This background, however, is well understood[9] and can be incorporated into a likelihood analysis. Consequently, similar improvements as in the case of searches for spin-independent interactions in $CaWO_4$ are expected.

### Additional science potential with CRESST detectors

**Bosonic dark matter: dark photons and ALPs.** Relic dark photons and ALPs, collectively referred to as dark bosons, are expected to be absorbed in cryogenic calorimeters followed by the emission of an electron carrying the incoming energy[16,45,46]. The expected signature of dark bosons is thus a mono-energetic electron recoil peak centered on the rest mass of the dark boson, with a width determined by the resolution of the detector. This spectral shape is distinct from the monotonically decaying energy spectrum of a potential LEE background. CRESST-III achieved energy thresholds down to 6.7 eV with a SOS detector[11] and down to 10 eV with a silicon detector[8] which correspond directly to the dark boson mass sensitivity. Preliminary studies based on the methods developed in ref. 47 demonstrate the feasibility of these searches in CRESST.

The future CRESST experiment has the potential to probe a new region of the bosonic DM mass range, specifically for dark photons and ALPs. To have a statistically significant observation of a peak above background, the larger exposure accessible with the upgraded setup will be required.

**Solar axions.** The potential of cryogenic bolometers for axion detection is demonstrated in ref. 14, which presents an experiment utilizing a $Tm_3Al_5O_{12}$ crystal to search for solar axions. This crystal contains $^{169}$Tm nuclei, which serve as targets for axion detection via resonant absorption. Given the demonstrated sensitivity of this method and its scalability, it is worth exploring the feasibility of incorporating solar axion searches as a new research avenue within the CRESST program. The upcoming upgrade of the CRESST experiment is expected to increase the number of simultaneously operating detectors, offering a promising platform for such investigations.

The $Tm_3Al_5O_{12}$ crystals would allow to simultaneously search for light DM and solar axions interactions opening the possibility of different DM-model studies inside CRESST. By utilizing the CRESST facility at LNGS, the extensive shielding that protects against environmental and cosmic radiation is likely to reduce background noise, thereby enhancing the sensitivity to solar axions.

## Long term vision

A long-term vision involves the possibility of using a large array of low-threshold cryogenic detectors in a next-generation rare event search. Such an experiment would have a rich scientific program and address several key scientific objectives, including direct DM detection, axion searches, and precision measurements of coherent elastic neutrino-nucleus scattering (CE$\nu$NS). The key enabler for such a broad physics program is the development of low-threshold detectors (sensitive to energies of $\mathcal{O}(1)\,eV$), the use of diverse nuclides as targets, high exposure, exceptional detector stability, and low background. These objectives require the low-threshold rare event search community to join efforts and they align closely with the overall goals of the future CRESST program.

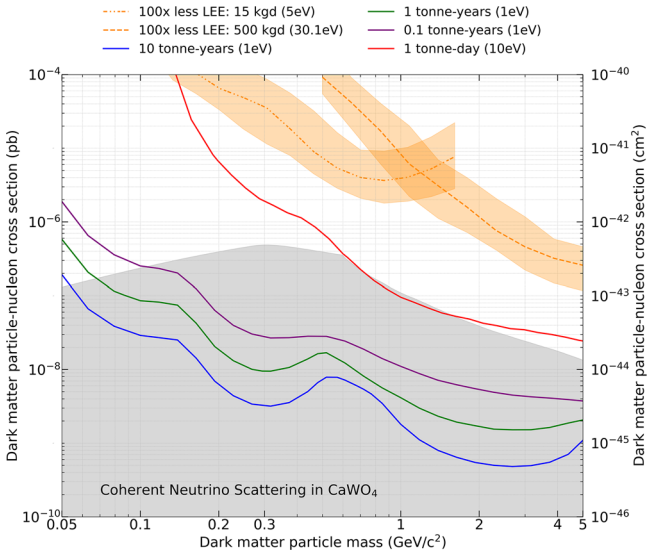


**Fig. 7 | Discovery potentials for dark matter in different experimental settings.** The four lower curves represent the 3$\sigma$ discovery potential for spin-independent DM-nucleus scattering in the presence of solar neutrinos and no other backgrounds, assuming various exposures and thresholds. Below these curves, due to neutrinos presence a DM discovery becomes impossible. CRESST after the upgrade is expected to remain approximately two orders of magnitude above the neutrino fog, assuming detector thresholds of 30.1 eV. The upper curve (orange) is the sensitivity projection for the CRESST upgrade assuming a 100 times less LEE with 515 kg · day exposure (26 detectors of 2 g with 5 eV threshold (double dash double dotted) and 70 detectors of 23.6 g with 30.1 eV threshold (dashed) in 1 year of data taking). The gray region highlights the so-called neutrino fog, calculated for $CaWO_4$ in ref. 48.

Simulations conducted for the next-generation of cryogenic solid-state experiments[48] indicate that a 1 tonne · day exposure of $CaWO_4$ with no LEE and $\mathcal{O}(10)$ eV threshold could start detecting solar neutrino events in the case of zero background as can be seen in Fig. 7. From this figure, it is clear that CRESST will remain approximately two orders of magnitude above the neutrino fog if the background is not further reduced and the exposure increased. Additionally lowering the threshold will further expand the accessible neutrino signal region. Reaching a 1 eV threshold together with a background reduction of the order of 10 within the next decade with this technology is a key objective of the CRESST Collaboration. In this scenario, neutrino events will start to play an important role in the background of CRESST.

The upcoming phase of CRESST experiment is expected to reach a total exposure of 1 tonne · day after a three-year data-taking period. If DM is not discovered and CRESST proceeds with a follow-up upgrade with increased exposure, decreased background and lower thresholds, the experiment could probe the neutrino fog. To achieve this goal, future advancements in detector multiplexing, background mitigation, and threshold reduction will drive CRESST's progress towards its long-term goals of being sensitive to DM in a region where neutrino interactions play an important role.

## Conclusion

The CRESST Collaboration presents an ambitious yet feasible upgrade plan to design, hall build, and operate the experiment in the coming years. This new phase of the CRESST program will feature ~100

detectors, each with a threshold between about 5 eV and 30 eV, and plans an exposure of at least 500 kg · day. This configuration is expected to enable sensitivity to cross sections as low as $\mathcal{O}(10^{-43})\,cm^2$ and to DM masses below 100 MeV/$c^2$.

While great progress has been achieved in elucidating the origin and pursuing the reduction of the LEE, these efforts are still ongoing, and further notable improvements are anticipated. But even in case the LEE cannot be fully eliminated, the CRESST experiment can deliver leading results. Classification of events occurring exclusively at the interface between the target and a sensor has been demonstrated already with new detector module designs. This enables the rejection of excess events that are localized at such interfaces, in contrast to DM events which are expected to interact uniformly throughout the target bulk. By employing a time-dependent LEE model in a likelihood-based framework, the impact of the LEE on the experiment's sensitivity can be even further reduced. Moreover, as the LEE decays over time, after 1.5 years of operation a tenfold reduction in the LEE is anticipated, providing a cross section sensitivity that improves over CRESST-III results by more than two orders of magnitude after at most an additional year of data-taking. After 3 years of operation, a reduction factor of 100 is expected, further enhancing the sensitivity significantly. The CRESST upgrade phase will thus be highly sensitive to light DM with masses below 100 MeV/$c^2$ and will additionally have sensitivity to spin-dependent DM interactions, solar axions, dark photons and ALPs. If DM is not discovered during this program, the CRESST Collaboration plans to pursue additional upgrades to further improve the sensitivity to light DM, facilitate solar axion and relic dark boson studies, and enable precision measurements of solar neutrinos.

## Data availability

Data corresponding to Fig. 4 are available online at https://www.origins-cluster.de/odsl/dark-matter-data-center/available-datasets/cresst. Other data shown in this work can be provided by the authors upon request.

Received: 30 April 2025; Accepted: 17 December 2025;
Published online: 12 May 2026

## References

1. Feng, J. L. The WIMP paradigm: theme and variations. *SciPost Phys. Lect. Notes* **71**, https://scipost.org/10.21468/SciPostPhysLectNotes.71 (2023).
2. Lee, B. W. & Weinberg, S. Cosmological lower bound on heavy-neutrino masses. *Phys. Rev. Lett.* **39**, 165–168 (1977).
3. Smirnov, J. & Beacom, J. F. Tev-scale thermal wimps: unitarity and its consequences. *Phys. Rev. D* **100**, https://doi.org/10.1103/PhysRevD.100.043029 (2019).
4. Lin, T. Dark matter models and direct detection. *PoS. Proc. Sci.* **333**, 009 (2019).
5. Cirelli, M., Strumia, A. & Zupan, J. Dark matter. https://arxiv.org/abs/2406.01705 (2024).
6. Angloher, G. et al. Limits on WIMP dark matter using sapphire cryogenic detectors. *Astropart. Phys.* **18**, 43–55 (2002).
7. Mancuso, M. et al. Searches for light dark matter with the CRESST-III experiment. *J. Low. Temp. Phys.* **199**, 547–555 (2020).
8. Angloher, G. et al. Results on sub-GeV dark matter from a 10 eV threshold CRESST-III silicon detector. *Phys. Rev. D.* **107**, 122003 (2023). The results of a Si detector module of the CRESST-III experiment consisting of a thin wafer, the target, and a larger bulk detector were presented in this paper with an improved existing limits for DM masses below 160 MeV/$c^2$ by up to a factor of 20.
9. Angloher, G. et al. Testing spin-dependent dark matter interactions with lithium aluminate targets in CRESST-III. *Phys. Rev. D.* **106**, 092008 (2022).
10. Abdelhameed, A. H. et al. First results from the CRESST-III low-mass dark matter program. *Phys. Rev. D.* **100**, 102002 (2019).
11. Angloher, G. et al. First observation of single photons in a CRESST detector and new dark matter exclusion limits. *Phys. Rev. D.* **110**, 083038 (2024). The CRESST-III collaboration reports the first observation of single photons in a cryogenic detector and uses this ultra-low threshold measurement to set new exclusion limits on sub-GeV dark-matter interactions.
12. Angloher, G. et al. Light dark matter search using a diamond cryogenic detector. *Eur. Phys. J. C.* **84**, 324 (2024). The CRESST Collaboration reports the use of a cryogenic diamond detector with a threshold of 16.8 eV to set exclusion limits on elastic spin-independent dark-matter-carbon interactions down to a mass of 0.122 GeV/$c^2$.
13. Cozzini, C. et al. Detection of the natural alpha decay of tungsten. *Phys. Rev. C.* **70**, 064606 (2004).
14. Abdelhameed, A. H. et al. New limits on the resonant absorption of solar axions obtained with a $^{169}$Tm-containing cryogenic detector. *Eur. Phys. J. C.* **80**, 376 (2020).
15. Mitridate, A., Trickle, T., Zhang, Z. & Zurek, K. M. Dark matter absorption via electronic excitations. *J. High. Energy Phys.* **2021**, 123 (2021).
16. Angloher, G. et al. Dark-photon search using data from CRESST-II phase 2. *Eur. Phys. J. C.* **77**, 299 (2017).
17. Angloher, G. et al. Constraints on self-interaction cross-sections of dark matter in universal bound states from direct detection. *Eur. Phys. J. C.* **84**, 1170 (2024).
18. Angloher, G. et al. Optimal operation of cryogenic calorimeters through deep reinforcement learning. *Comput. Softw. Big Sci.* **8**, 10 (2024).
19. Angloher, G. et al. Towards an automated data cleaning with deep learning in CRESST. *Eur. Phys. J.* **138**, 100 (2023.
20. Angloher, G. et al. High-dimensional Bayesian likelihood normalisation for CRESST's background model. *JINST* **19**, P11013 (2024).
21. Adari, P. et al. EXCESS workshop: Descriptions of rising low-energy spectra. *SciPost Phys. Proc*. 001, https://scipost.org/10.21468/SciPostPhysProc.9.001 (2022).
22. Angloher, G. et al. Latest observations on the low energy excess in CRESST-III. *SciPost Phys. Proc*. 013, https://scipost.org/10.21468/SciPostPhysProc.12.013 (2023).
23. Baxter, D. et al. Low-energy backgrounds in solid-state phonon and charge detectors. *Annu. Rev. Nucl. Part. Sci.* https://doi.org/10.1146/annurev-nucl-121423-100849 (2025).
24. Angloher, G. et al. DoubleTES detectors to investigate the CRESST low energy background: results from above-ground prototypes. *Eur. Phys. J. C.* **84**, 1001 (2024). [Erratum: Eur.Phys.J.C 84, 1227 (2024)].
25. Karl, A. *Simulation Based Background Comparison of Future Detector Modules of the CRESST Experiment*. Master's thesis, TU Wien (2022).
26. Angloher, G. et al. Detector development for the CRESST experiment. *J. Low. Temp. Phys.* **216**, 393–401 (2024).
27. Collaboration, C. A short history of cresst. Accessed 17 April 2025. https://cresst-experiment.org/the-cresst-experiment/a-short-history-of-cresst (2025).
28. Angloher, G. et al. Limits on WIMP dark matter using scintillating $CaWO_4$ cryogenic detectors with active background suppression. *Astropart. Phys.* **23**, 325–339 (2005).
29. Angloher, G. et al. Commissioning run of the CRESST-II dark matter search. *Astropart. Phys.* **31**, 270–276 (2009).
30. Angloher, G. et al. Results from 730 kg days of the CRESST-II dark matter search. *Eur. Phys. J. C.* **72**, 1971 (2012).
31. Angloher, G. et al. Results on low mass WIMPs using an upgraded CRESST-II detector. *Eur. Phys. J. C.* **74**, 3184 (2014).
32. Angloher, G. et al. Probing low WIMP masses with the next generation of CRESST detector. arXiv: https://doi.org/10.48550/arXiv.1503.08065 (2015).
33. Strauss, R. et al. Energy-dependent light quenching in $CaWO_4$ crystals at mK temperatures. *Eur. Phys. J. C.* **74**, 2957 (2014).
34. Angloher, G. et al. A likelihood framework for cryogenic scintillating calorimeters used in the CRESST dark matter search. *Eur. Phys. J. C.* **84**, 922 (2024).

35. Abdelhameed, A. H. et al. Geant4-based electromagnetic background model for the CRESST dark matter experiment. *Eur. Phys. J. C.* **79**, 881 (2019). [Erratum: *Eur. Phys. J. C* **79**, 987 (2019)].
36. Wulandari, H. et al. Neutron flux at the Gran Sasso underground laboratory revisited. *Astropart. Phys.* **22**, 313–322 (2004).
37. Strauss, R. et al. A detector module with highly efficient surface-alpha event rejection operated in CRESST-II Phase 2. *Eur. Phys. J. C.* **75**, 352 (2015).
38. Zema, V. Excess workshop 2022/2023. Presented at the EXCESS Workshop (2023). Workshop presentation "The low energy excess in CRESST-III" https://indico.cern.ch/event/1213348/contributions/5411385/.
39. Anthony-Petersen, R. et al. A stress-induced source of phonon bursts and quasiparticle poisoning. *Nat. Commun.* **15**, 6444 (2024).
40. Stahlberg, M. *Probing Low-Mass DarkMatter with CRESST-III—Data Analysis and First Results*. Ph.D. thesis, TU Wien (2021).
41. Adams, D. Q. et al. Search for Majorana neutrinos exploiting millikelvin cryogenics with CUORE. *Nature* **604**, 53–58 (2022).
42. Einfalt, L. *Light Quenching in Scintillator-Based Cryogenic Detectors for Dark Matter Searches*. Ph.D. thesis, TU Wien (2024).
43. Kinast, A. et al. Improving the quality of $CaWO_4$ target crystals for CRESST. *J. Low. Temp. Phys.* **209**, 1128–1134 (2022).
44. Strauss, R. et al. Beta/gamma and alpha backgrounds in CRESST-II Phase 2. *J. Cosmol. Astropart. Phys*. **06**, 030 (2015).
45. An, H., Pospelov, M., Pradler, J. & Ritz, A. Direct detection constraints on dark photon dark matter. *Phys. Lett. B* **747**, 331–338 (2015).
46. Hochberg, Y., Lin, T. & Zurek, K. M. Absorption of light dark matter in semiconductors. *Phys. Rev. D.* **95**, 023013 (2017).
47. Zema, V. et al. Dark matter-electron scattering search using cryogenic light detectors. *Phys. Rev. D.* **110**, 123012 (2024).
48. Bento, A. et al. Solar neutrinos in cryogenic detectors. *Eur. Phys. J. C.* **84**, 1118 (2024).
49. Liu, Z. Z. et al. Constraints on spin-independent nucleus scattering with sub-GeV weakly interacting massive particle dark matter from the CDEX-1B experiment at the China Jinping Underground Laboratory. *Phys. Rev. Lett.* **123**, 161301 (2019).
50. Agnese, R. et al. Search for low-mass dark matter with CDMSlite using a profile likelihood fit. *Phys. Rev. D.* **99**, 062001 (2019).
51. Aguilar-Arevalo, A. et al. Results on low-mass weakly interacting massive particles from a 11 kg-day target exposure of DAMIC at SNOLAB. *Phys. Rev. Lett.* **125**, 241803 (2020).
52. Hehn, L. et al. Improved EDELWEISS-III sensitivity for low-mass WIMPs using a profile likelihood approach. *Eur. Phys. J. C.* **76**, 548 (2016).
53. Agnese, R. et al. Search for low-mass weakly interacting massive particles with SuperCDMS. *Phys. Rev. Lett.* **112**, 241302 (2014).
54. Alkhatib, I. et al. Light dark matter search with a high-resolution athermal phonon detector operated above ground. *Phys. Rev. Lett.* **127**, 061801 (2021).
55. Albakry, M. F. et al. Investigating the sources of low-energy events in a SuperCDMS-HVeV detector. *Phys. Rev. D.* **105**, 112006 (2022).
56. Agnes, P. et al. Search for low-mass dark matter WIMPs with 12 ton-day exposure of DarkSide-50. *Phys. Rev. D.* **107**, 063001 (2023).
57. Li, S. et al. Search for light dark matter with ionization signals in the PandaX-4T experiment. *Phys. Rev. Lett.* **130**, 261001 (2023).
58. Ma, W. et al. Search for solar B8 neutrinos in the PandaX-4T experiment using neutrino-nucleus coherent scattering. *Phys. Rev. Lett.* **130**, 021802 (2023).
59. Aprile, E. et al. First search for light dark matter in the neutrino fog with XENONnT. *Phys. Rev. Lett.* **134**, 111802 (2025).
60. Collar, J. I. Search for a nonrelativistic component in the spectrum of cosmic rays at Earth. *Phys. Rev. D.* **98**, 023005 (2018).
61. Arnaud, Q. et al. First results from the NEWS-G direct dark matter search experiment at the LSM. *Astropart. Phys.* **97**, 54–62 (2018).
62. Amole, C. et al. Dark matter search results from the complete exposure of the PICO-60 $C_3F_8$ bubble chamber. *Phys. Rev. D.* **100**, 022001 (2019).


## Acknowledgements

This work has been funded in part by the Deutsche Forschungsgemeinschaft (DFG, German Research Foundation) under Germany's Excellence Strategy - EXC 2094 - 390783311 and through the Sonderforschungsbereich (Collaborative Research Center) SFB1258 "Neutrinos and Dark Matter in Astro- and Particle Physics", by the BMBF 05A20WO1 and 05A20VTA, by the Austrian Science Fund (FWF) https://doi.org/10.55776/PAT1239524 and by https://doi.org/10.55776/I5420. J. Burkhart and H. Kluck. were funded through the FWF project 10.55776/P34778 "ELOISE". The Bratislava group acknowledges a partial support provided by the Slovak Research and Development Agency (projects APVV-15-0576 and APVV-21-0377).

## Author contributions

All authors have contributed to the publication, being variously involved in designing the detector, writing offline software, performing simulations and data analysis, discussing and approving the scientific results. This article was prepared by a subgroup of authors appointed by the CRESST collaboration. The manuscript was produced by P.V. Guillaumon, V. Mokina and B.v. Krosigk. Figure 2 and 3 were done by V. Mokina, Figs. 4–6 were done by F. Dominsky and Fig. 7 by D. Fuchs. All authors have read and agreed to the published version of the manuscript. Authors are listed alphabetically by their last names.

## Funding

Open Access funding enabled and organized by Projekt DEAL.

## Competing interests

L.C. is a Guest Editor for Communications Physics, but was not involved in the editorial review of, or the decision to publish this article. All other authors declare no competing interests, where relevant.

## Additional information

**Correspondence** and requests for materials should be addressed to F. Dominsky, P. V. Guillaumon, B. V. Krosigk or V. Mokina.

**Peer review information** *Communications Physics* thanks Timothée Hessel and the other, anonymous, reviewer(s) for their contribution to the peer review of this work.

[1]Max-Planck-Institut für Physik, Garching bei München, Germany. [2]Institut für Hochenergiephysik der Österreichischen Akademie der Wissenschaften, Wien, Austria. [3]Atominstitut, Technische Universität Wien, Wien, Austria. [4]Kirchhoff-Institute for Physics, Heidelberg University, Heidelberg, Germany. [5]Faculty of Mathematics, Physics and Informatics, Comenius University, Bratislava, Slovakia. [6]INFN, Laboratori Nazionali del Gran Sasso, Assergi, Italy. [7]Eberhard-Karls-Universität Tübingen, Tübingen, Germany. [8]Physik-Department, TUM School of Natural Sciences, Technische Universität München, Garching, Germany. [9]Department of Physics, University of Oxford, Oxford, UK. [10]Institute for Astroparticle Physics, Karlsruhe Institute of Technology, Karlsruhe, Germany. [11]Present address: LIBPhys, Departamento de Fisica, Universidade de Coimbra, Coimbra, Portugal. [12]Present address: Dipartimento di Fisica, Università di Milano Bicocca, Milano, Italy. [13]Present address: School of Physics, The University of Melbourne, Melbourne, VIC, Australia. [14]Present address: ARC Centre of Excellence for Dark Matter Particle Physics, Melbourne, VIC, Australia. [15]Present address: Walther-Meißner-Institut für Tieftemperaturforschung, Garching, Germany. [16]Present address: Instituto de Física da Universidade de São Paulo, São Paulo, Brazil. [17]Present address: Dipartimento di Ingegneria Civile e Meccanica, Università degli Studi di Cassino e del Lazio Meridionale, Cassino, Italy. ✉e-mail: dominsky@mpp.mpg.de; pedro.guillaumon@mpp.mpg.de; bkrosigk@kip.uni-heidelberg.de; valentyna.mokina@oeaw.ac.at